# *Supplement to* Urban ozone formation and sensitivities to volatile chemical products, cooking emissions, and $NO_x$ across the Los Angeles Basin

Chelsea E. Stockwell[1]*, Matthew M. Coggon[1], Rebecca H. Schwantes[1], Colin Harkins[1,2], Bert Verreyken[1,a,b], Congmeng Lyu[1,2], Qindan Zhu[1,2,c], Lu Xu[1,2,d], Jessica B. Gilman[1], Aaron Lamplugh[1,2,e], Jeff Peischl[1,2,f], Michael A. Robinson[1,2], Patrick R. Veres[1,g], Meng Li[1,2], Andrew W. Rollins[1], Kristen Zuraski[1,2], Sunil Baidar[1,2], Shang Liu[3], Toshihiro Kuwayama[4], Steven S. Brown[1], Brian C. McDonald[1], Carsten Warneke[1]

[1] NOAA Chemical Sciences Laboratory, Boulder, CO, 80305, USA

[2] Cooperative Institute for Research in Environmental Sciences, University of Colorado Boulder, Boulder, CO, 80309, USA

[3] Department of Civil and Environmental Engineering, Northeastern University, Boston, MA, 02115, USA

[4] California Air Resources Board, Sacramento CA USA

[a] now at: Royal Belgian Institute for Space Aeronomy (BIRA-IASB), Brussels, Belgium

[b] now at: Biosystems Dynamics and Exchanges (BIODYNE), Gembloux Agro-Bio Tech, University of Liege, Liege, Belgium

[c] now at: Department of Earth, Atmospheric and Planetary Sciences, Massachusetts Institute of Technology, Cambridge, MA,
United States

[d] now at: Department of Energy, Environmental and Chemical Engineering, Washington University in St. Louis, Missouri, USA

[e] now at: Technical Services Program, Air Pollution Control Division, Colorado Department of Public Health and Environment, Denver, CO USA

[f] now at: NOAA Global Monitoring Laboratory, Boulder, CO, 80305, USA

[g] now at: National Center for Atmospheric Research, Boulder, Colorado, USA

*Correspondence to*: Chelsea Stockwell (Chelsea.Stockwell@noaa.gov)

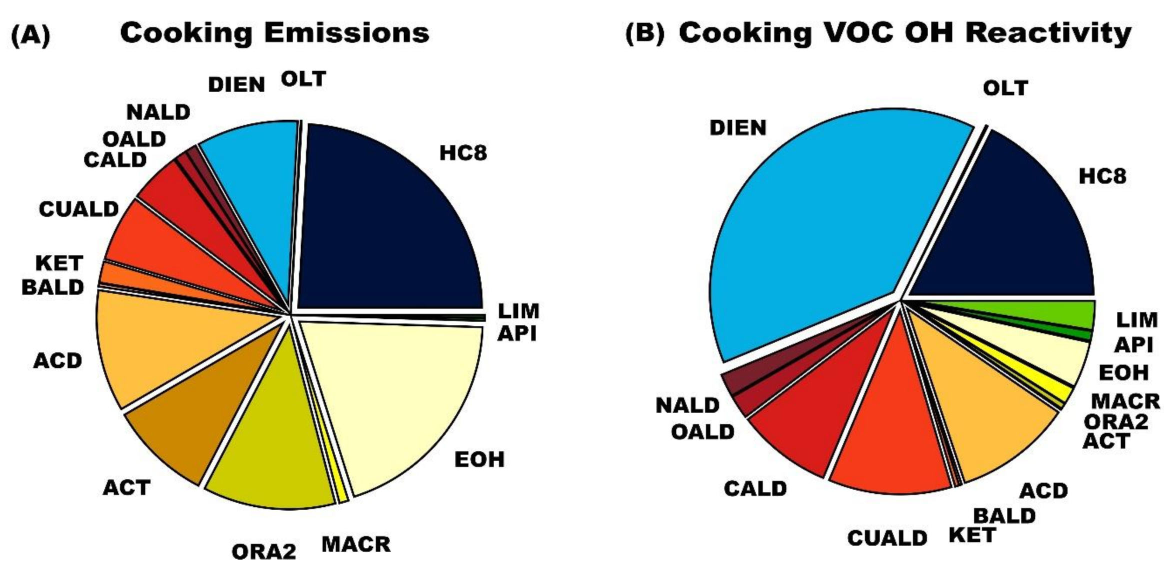

**Figure S1:** (A) The FIVE-VCP-NEI17NRT cooking emissions mapped to RACM2B-VCP species following the definition scheme outlined in Goliff et al. (2013). Chemical species added to the RACM2B-VCP mechanism include cooking saturated aldehydes (CALD), cooking unsaturated aldehydes (CUALD), octanal (OALD), and nonanal (NALD). (B) The lumped estimated VOC OH reactivity from cooking.

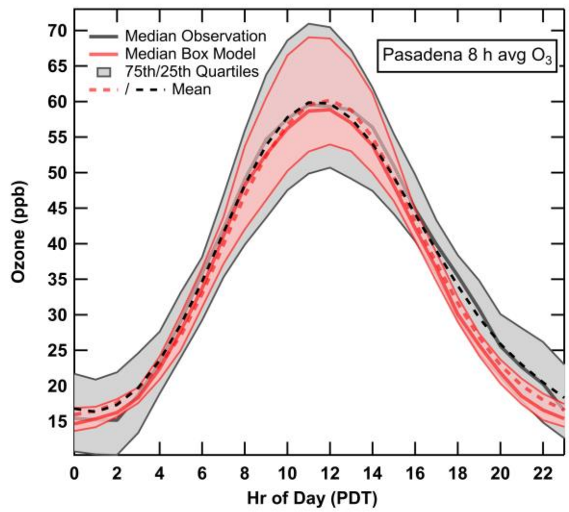


**Figure S2:** The median diel profile of the moving mean 8 h ozone (grey line) overlaid with box model output (red line) in Pasadena, CA. The mean is a dashed line and the median is marked by the solid. Shaded regions indicate the 75th and 25th quartile ranges.

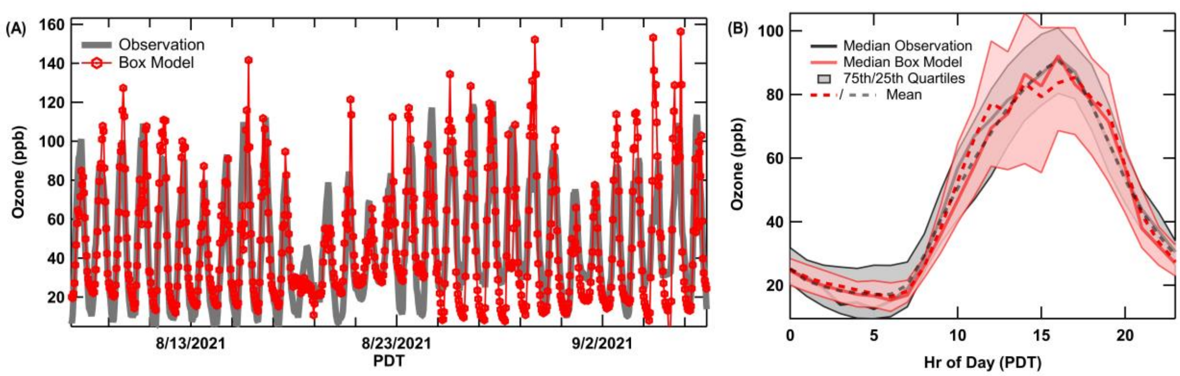


**Figure S3:** (A) The observed ozone time series (grey lines) overlaid with box model output (red markers) from 7 August – 7 September in Redlands, CA. (B) The median diel profile of modeled (red) and measured (grey) ozone in Redlands, CA. The mean is a dashed line and the median is marked by the solid. Shaded regions indicate the 75th and 25th quartile ranges.

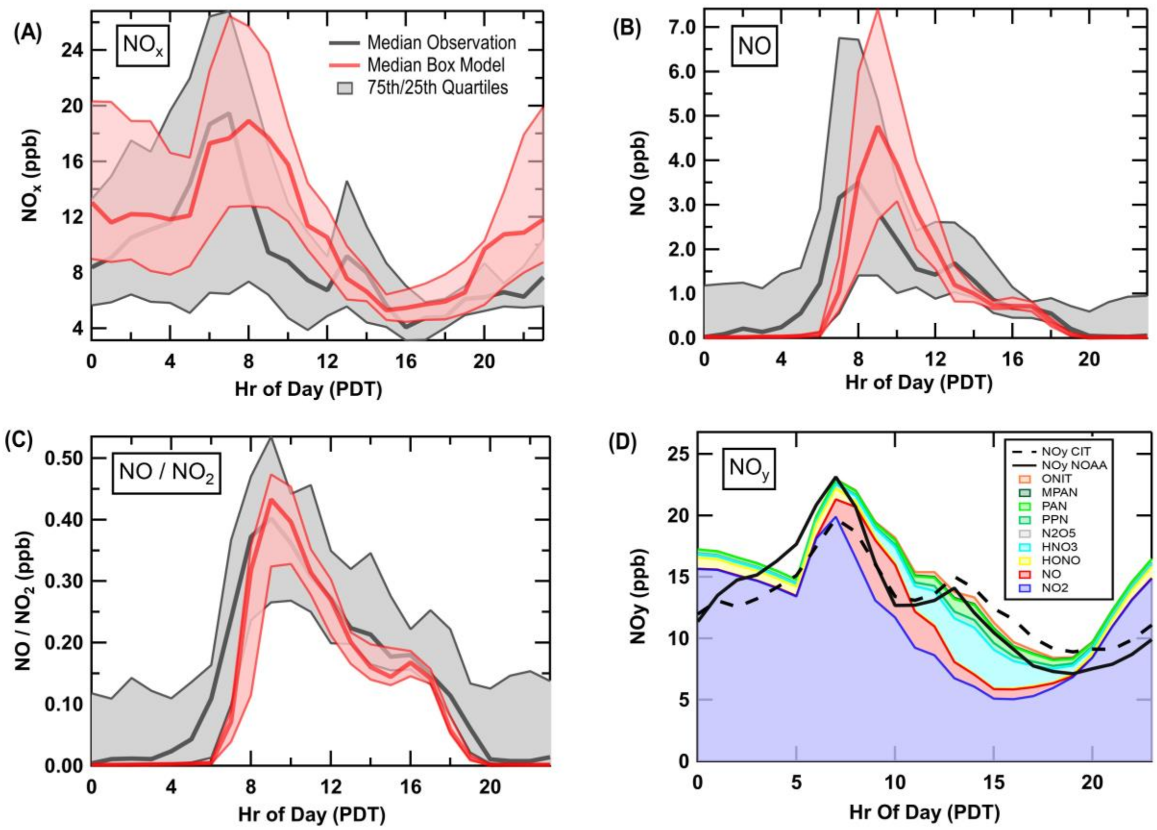


**Figure S4:** (A) The median diel profile $NO_x$ (grey line) overlaid with box model output (red line). The mean is a dashed line and the median is marked by the solid line with shaded regions indicating the 75th and 25th quartile ranges. The median diel profile of (B) NO and (C) NO to $NO_2$ observations (grey) and model output (red). (D) The additive model output of speciated nitrogen compounds overlaid with the average $NO_y$ measurements from the SUNVEx ground site ($NO_y$ NOAA; solid black) and the Linde Laboratory ($NO_y$ CIT; dashed black), both in Pasadena, CA.

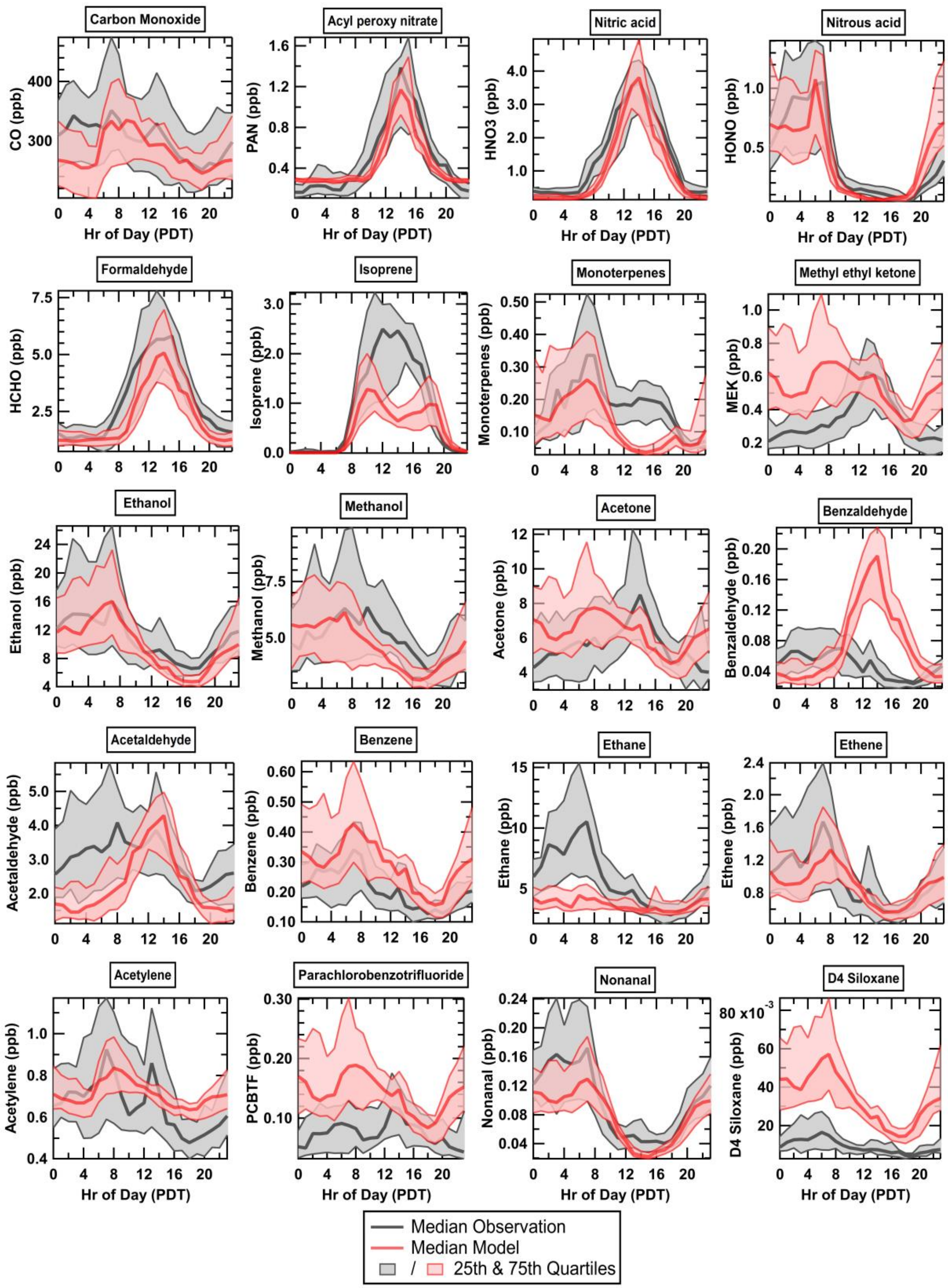


**Figure S5:** (A) The median diel profiles (grey) overlaid with box model results (red) for overlapping species modeled explicitly in the RACM2B-VCP mechanism scheme. The shaded regions indicate the 75th and 25th quartile ranges.

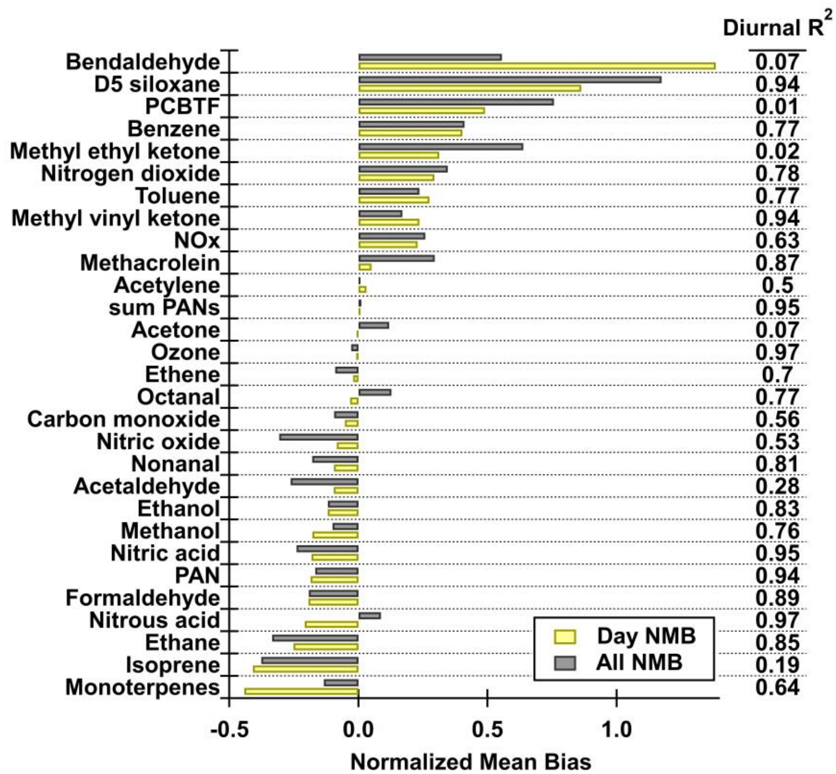


**Figure S6:** The box model normalized mean bias (NMB) and correlation coefficient ($R^2$) for explicit species in RACM2B-VCP that overlap with observations. The hourly NMB is calculated following Eq. 3 for all data (grey) and for daylight hours only (7:00-19:00 LT; yellow).

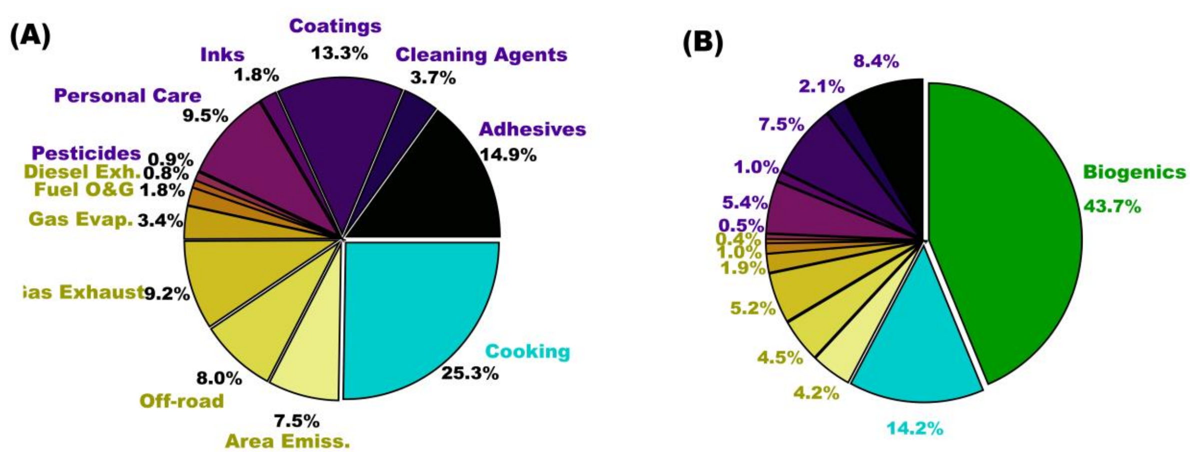


**Figure S7:** The fractional contribution to MDA8 ozone in Redlands, CA from: (A) anthropogenic VOC sources including VCPs (purple shading), fossil fuels (yellow shading), and cooking (blue) emissions. (B) anthropogenic plus biogenic VOCs.

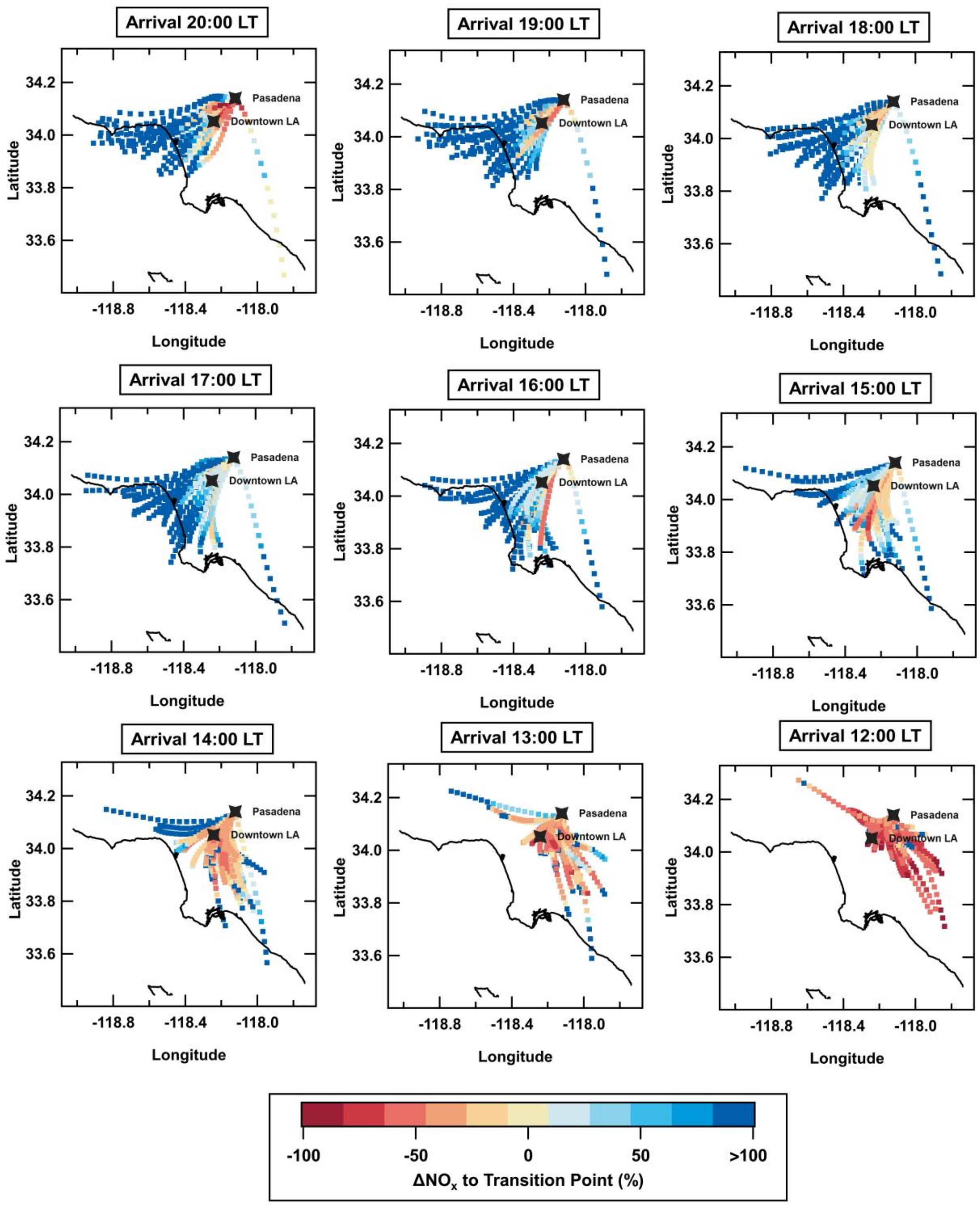


**Figure S8:** Trajectories arriving in Pasadena between 12:00-20:00 LT colored by the percent change in $NO_x$ needed to transition between photochemical regimes. Warmer colors (-%) indicate the location is currently $NO_x$–saturated, while cooler (+%) is $NO_x$–limited.

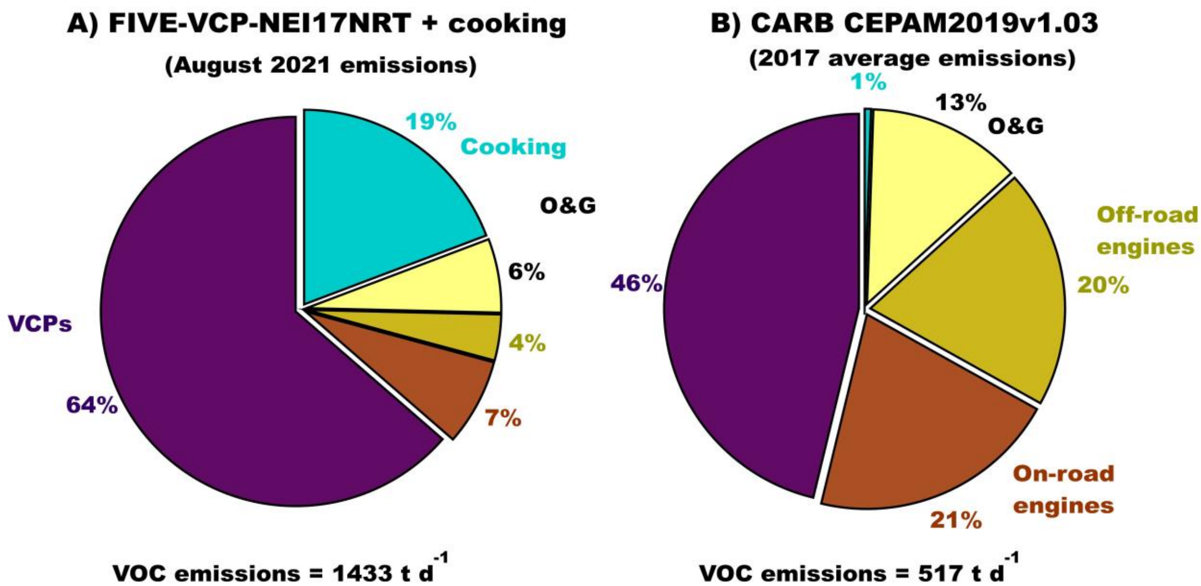


**Figure S9:** Distribution of VOC emissions in the South Coast Air Basin from the (A) FIVE-VCP-NEI17NRT inventory for August, 2021 and (B) CARB CEPAM2019v1.03 tool that represents annual emissions for 2017. Note: In the FIVE-VCP-NEI17NRT inventory, base cooking emission estimates were used, and cooking ethanol was not adjusted to align with aircraft flux measurements as outlined in Section 2.2.2.

| Reaction | Rates & reaction coefficients |
|---|---|
| CALD+NO3=0.22 HC5P+0.78 RCO3+HNO3+PHNO3+LNOXHNO3 | 1.60E-14 |
| CUALD+NO3=MACP+HNO3+PHNO3+LNOXHNO3 | 3.40E-15 |
| CUALD+O3=0.902 MGLY+0.242 HCHO+0.238 HO+0.652 CO+0.098 RCO3+0.204 ORA1+0.14 HO2+0.144 H2O2 | 1.4e-15*exp(-2100.0 / T ) |
| CALD+HO=0.19 HC5P+0.81 RCO3+H2O+OHR+OHVOC | 7.23e-12*exp(410.0 / T ) |
| CUALD+HO=0.53 MACP+0.47 UALP+OHR+OHVOC | 8.0e-12*exp(380.0 / T ) |
| CUALD+hv=0.5 MACP+0.175 RCO3+0.5 HCHO+0.325 ETHP+0.825 CO+HO2 | JMACR |
| CALD+hv=HC5P+HO2+CO | JALD |
| OALD+hv=HC8P+HO2+CO | JALD |
| NALD+hv=HC8P+HO2+CO | JALD |
| OALD+NO3=0.2 HC8P+0.8 RCO3+HNO3+PHNO3+LNOXHNO3 | 1.70E-14 |
| OALD+HO=0.14 HC8P+0.86 RCO3+H2O+OHR+OHVOC | 7.78e-12*exp(410.0 / T ) |
| NALD+NO3=0.19 HC8P+0.81 RCO3+HNO3+PHNO3+LNOXHNO3 | 2.00E-14 |
| NALD+HO=0.15 HC8P+0.85 RCO3+H2O+OHR+OHVOC | 8.08e-12*exp(410.0 / T ) |

**Table S1:** Added reactions for cooking saturated aldehydes (CALD), cooking unsaturated aldehydes (CUALD), octanal (OALD), and nonanal (NALD). Additional species identifiers can be found in Goliff et al. (2013).

## References

Goliff, W. S., Stockwell, W. R., and Lawson, C. V.: The regional atmospheric chemistry mechanism, version 2, Atmospheric Environment, 68, 174-185, https://doi.org/10.1016/j.atmosenv.2012.11.038, 2013.